npj | vaccines

Article

Published in partnership with the Sealy Institute for Vaccine Sciences

https://doi.org/10.1038/s41541-025-01110-3

Cytolytic γδ T-cells and IFNγ-producing CD4-lymphocytes characterise the early response to MTBVAC tuberculosis vaccine

María-José Felgueres[1], Gloria Esteso[1,6], Álvaro F. García-Jiménez[1,6], Alberto Benguría[2], Enrique Vázquez[2], Nacho Aguiló[3], Eugenia Puentes[4], Ana Dopazo[2,5], Ingrid Murillo[4], Carlos Martín[3], Esteban Rodríguez[4], Hugh T. Reyburn[1] & Mar Valés-Gómez[1] ✉

Infection with *Mycobacterium tuberculosis* (Mtb) can produce a wide spectrum of clinical manifestations, ranging from active tuberculosis (TB) to asymptomatic latent infection. Although CD4 T-cells are key immune effectors to control TB, early after infection, the innate immune response must play a role in tackling the disease. Here, we performed in-depth analyses of the acute immune response to MTBVAC, a candidate vaccine engineered from Mtb with the aim of protecting adults from pulmonary TB disease, still a major global challenge. scRNA-seq shows expansion of $CD4^+$ and cytotoxic γδ T-cells, data confirmed by flow cytometry. CD4 T-cells exhibited lower HLA-DR and higher L-selectin expression, compared to BCG-stimulation, indicating differential activation or dynamics. Importantly, MTBVAC-activated γδ T-cells had a unique cytotoxic $CD16^+GZMB^+$ phenotype, reminiscent of effector cells found in Mtb positive individuals controlling infection. IFN-γ and TNF-α were released in cultures, while IL-17A/F were almost undetectable.

Despite the discovery over a century ago of *Mycobacterium tuberculosis* (Mtb), tuberculosis (TB) epidemics are still a major global health problem, according to WHO, mainly due to the lack of identification of infected persons and, therefore, lack of preventive therapy[1]. In addition, the COVID-19 pandemic disrupted TB services, resulting in an estimated half a million excess TB deaths between 2020 and 2022. Since the decrease in TB deaths was only 19% between 2015 and 2022, far below the WHO End TB Strategy's 2025 milestone of a 75% reduction. Therefore, effective immunization against pulmonary TB remains an urgent need to eliminate this persistent infectious disease. The only licensed vaccine for TB is *bacillus Calmette-Guérin* (BCG), an attenuated bacterial strain derived from *Mycobacterium bovis*[2]. BCG protects against primary infection and several extrapulmonary manifestations of Mtb infection, like meningeal and miliary TB in children and infants[3]. However, BCG is less efficient in the prevention of pulmonary TB, in particular in adults[4]. For this reason, a global effort on the development of new TB vaccines is ongoing, with several candidates entering clinical trials[5]. Besides its use as TB vaccine, BCG is the standard of care therapy for non-muscle invasive bladder cancer, preventing progression in nearly 70% of patients[6].

MTBVAC is, unlike most TB vaccines that are based on *M. bovis*, a live-attenuated vaccine engineered from Mtb to eliminate two independent virulence genes, *phoP* and *fadD26*. This design was conceived to create, in a safe background, a genetically stable variant of Mtb that might lead to more specific and longer lasting immune responses[7]. MTBVAC has proven to be safe and effective, in animal models and clinical trials[8,9]. Orthotopic mouse models of bladder cancer indicate a greater therapeutic effect of MTBVAC compared to BCG[10]. Currently, MTBVAC is being tested in Phase 3 efficacy trials, in newborns from TB-endemic countries.

It has been estimated that 90% of infections result in a latent TB infection (LTBI), where there is immune control of Mtb, as compared to

[1]Department of Immunology and Oncology, National Centre for Biotechnology, Spanish National Research Council (CNB-CSIC), Madrid, Spain. [2]Genomics Unit, Centro Nacional de Investigaciones Cardiovasculares (CNIC), Madrid, Spain. [3]Department of Microbiology, Pediatrics, Radiology and Public Health of the University of Zaragoza and Centro Investigación en Red de Enfermedades Respiratorias CIBERES, ISCIII, Zaragoza, Spain. [4]Clinical Research and Research & Development Departments, Biofabri, Zendal Group, O'Porriño, Pontevedra, Spain. [5]CIBER de Enfermedades Cardiovasculares, (CIBERCV), Madrid, Spain. [6]These authors contributed equally: Gloria Esteso, Álvaro F. García-Jiménez.
✉e-mail: mvales@cnb.csic.es

active TB disease[11,12] which is contagious in adults. Concurring with the broad spectrum of TB's clinical manifestations[13], many immune aspects are involved in TB control and clearance, and not all are completely understood[12], for example, the relationship between T lymphocyte activation and progression of the disease is unclear[14]. CD4 T-cells secrete IFN-γ, TNF-α, and/or IL2 which can activate macrophages and CD8 T-cells, for anti-bacterial activity. Non-donor restricted T-cells, such as NKT cells, γδ T-cells and mucosal associated invariant T-cells (MAITs), as well as Natural Killer (NK) and other innate-like lymphocytes (ILCs), present in the airways of humans, can also play important roles in TB as first defence immune agents. NK cell activation and proliferation are involved in TB latency[15], while γδ T-cells can play pleiotropic roles, ranging from effector IFN-γ-producing cells to suppressor IL-17 secretion[16,17]. A $CD8^+$ $CD16^+$ subtype of effector memory γδ T-cells has been described in South African adolescents with latent Mtb infection[18]. In contrast, patients with active pulmonary disease have more circulating IL-17-producing γδ T-cells than healthy donors[19], perhaps suggesting a role for IL-17 in pathology.

With respect to the immune response generated by MTBVAC, evaluation of cytokine-producing CD4 T-cell populations has been measured in both non-human primate experiments and in individuals included in clinical trials from week 4 after immunization[9,20]. However, the study of the initial interactions of MTBVAC with human innate lymphocytes has not yet been evaluated in detail. Data on human monocytes 24 h after exposure to the vaccine revealed release of the pro-inflammatory cytokines IL-1β, IL-6 and TNF-α[21]. Understanding these early interactions may help to gain insight into the processes involved in the success of this TB vaccine, as well as to predict events like resistance, elimination and/or tolerance of the mycobacteria.

Here, we studied in detail the proliferation and phenotype of lymphocytes expanded after co-culture of human peripheral blood mononuclear cells (PBMC) with MTBVAC. Besides the Th1 CD4 T-cell population, a subpopulation of effector γδ T-cells with an IFN-γ and cytotoxic profile clearly proliferated. From the anti-cancer perspective, MTBVAC did not stimulate a predominant NK cell response, however, cytotoxicity of MTBVAC-primed PBMC against bladder cancer cells was observed, as well as a clear NK cell degranulation. Previous in vivo research, together with these data, suggests that MTBVAC vaccine might eliminate tumours using mechanisms other than NK cell cytotoxicity.

Results

Proliferation of $CD4^+$ and γδ T-cells after culture of PBMC with MTBVAC

PBMC from three healthy donors were incubated with either MTBVAC or BCG-Moreau RJ strain (iBCG), without exogenous addition of cytokines and, 7 days later, cells were recovered for either single cell RNA sequencing (scRNA-seq) or FACS analyses. A first scRNA-seq analysis of this dataset was done including paired data obtained in parallel for iBCG[22] and MTBVAC (Quality control in Supplementary Fig. 1). Large proportions of activated lymphocyte populations, mainly CD4 and γδ T-cells, were identified 7 days after exposure to both vaccines (Fig. 1a, Supplementary Fig. 2), and these data were confirmed by flow cytometry (Fig. 1b, Supplementary Fig. 3) and in proliferation experiments (Fig. 1c). Initial inspection indicated a similar lymphocyte population distribution with both vaccines. Interestingly, compared to iBCG, more CD4 T-cells and less γδ T-cells expanded with MTBVAC. Although CD8 T-cells and NK cells were minority populations, the scRNA-seq data indicated that, together with CD4 and γδ T-cells, they had clear cytotoxic and effector potential, as shown by expression of GZMB, TNFSF10, FASLG, IFNG (Supplementary Fig. 2).

Although in the initial scRNA-seq analysis cell groups converged in the same cluster based on sharing a certain number of genes, this does not mean they are 100% identical[23]. Indeed, when scRNA-seq data of MTBVAC-stimulated PBMC were studied individually in depth to gain detailed insight into this immune response (Fig. 2; quality criteria Supplementary Fig. 1), 12 clusters defined by differential gene expression were identified and annotated (Fig. 2a, b, Supplementary Fig. 4). MTBVAC-stimulated PBMC yielded 3 clusters of CD4 T-cells (clusters 2, 3, 4) and 3 clusters within a large γδ T-cell population (clusters 1, 6, 8).

CD4 T-cell phenotypes after 7-day exposure to MTBVAC

Cytokine-producing CD4 T-cells are thought to play a key role in the control of Mtb infection. Thus, differential gene expression of the three distinct CD4 T-cell clusters (C2: naïve, C3: memory, C4: activated) that were present following MTBVAC co-culture was analysed (Fig. 2). As previously described for other mycobacteria, the phenotype of the activated CD4 population (C4) expanded with MTBVAC corresponds mainly with Th1, with increased RNA transcripts for CXCR3, IFNG and lytic granule components, as well as CCL5 (Fig. 3a). Further analysis of the activated Th1 cluster of CD4 T-cells revealed 2 clear subpopulations (Fig. 3b–d): SC1, enriched in IL7R and AQP3 (aquaporin-3), consistent with a memory, less activated subpopulation; while SC2 had markers consistent with a potent Th1 activation, displaying a strong expression of molecules like IFNG, CSF2, IL26 or TNF, but not IL17A.

Since there were similarities in the cell populations in MTBVAC and iBCG-stimulated PBMC, detailed analyses of the differences between the effector populations were carried out. For CD4 T-cells, the main differences between the two vaccines occurred in MHC class II gene expression (Fig. 3e): HLA-DP, DQ, DR and DM were less expressed after MTBVAC stimulation, while SELL [L-selectin (CD62L)] transcripts were only found in CD4 T cells activated by culture with MTBVAC, but not BCG. These findings could reflect differences in CD4 T cell activation after exposure to either MTBVAC or iBCG.

The phenotype of activated CD4 T-cells was confirmed by flow cytometry (Fig. 3f, g; Supplementary Fig. 5). As expected, the CD25 activated subset was negative for CD62L and expressed HLA-DR, while the CD62L-positive population was negative for HLA-DR and CD25. Moreover, a clear increase of CXCR3 was observed in activated CD4 T-cells after stimulation with both vaccines, iBCG and MTBVAC.

Altogether, MTBVAC stimulation activated a CD4 T-cell population with strong expression of MHC-II, presumably proliferating after antigen encounter, and homing molecules like CXCR3.

MTBVAC stimulates $CD16^+GZMB^{hi}$ cytolytic γδ T-cells expressing CD62L

γδ T-cells have been proposed to play important roles in Mtb control[18]. In fact, three distinct γδ T-cell clusters (C1, C6, C8) (Fig. 2a) were observed to proliferate actively after MTBVAC stimulation. scRNA-seq analysis of the γδ T-cell population obtained after a 7-day incubation of PBMC with MTBVAC showed that these cells were mainly Vγ9Vδ2 (TRDV2, TRGV9) (Fig. 2b). Further in-depth analyses revealed 7 subclusters (Fig. 4a, Supplementary Fig. 6a), many of them expressing CD27 (Fig. 4b). Moreover, a marked expression of IFN-γ was found, especially in SC3, which represents an active subpopulation ($IL2RA^+IFNG^+$) (Fig. 4c). $CD27^+$ $IFNγ^+$ γδ T-cells have been described as pro-inflammatory with anti-tumour capacity, as opposed to suppressor $CD27^-$ $IL17A^+$ γδ T-cells[16]. As expected from the $CD27^+$ $IFNγ^+$ phenotype, MTBVAC-primed γδ T-cells did not express IL17A. In line with this, both TB vaccines, BCG and MTBVAC, stimulated γδ T-cells to express high levels of cytotoxic molecules like GZMM, GZMB and GNLY, proinflammatory chemokines like CCL5 (RANTES), and receptors like CXCR3 (Fig. 4d). Despite these similarities, transcriptomic analysis of γδ T-cells also identified some differences between MTBVAC and BCG-activated PBMC: MTBVAC stimulation led to more cells expressing molecules like HAVCR2 (TIM3) and TNFRSF9 (4-1BB), albeit at low levels. These molecules have been associated with either T-cell activation or exhaustion in different contexts[24–26]. So, while a low TIM3 expression could denote some level of exhaustion, proinflammatory and activation markers would argue against this possibility for γδ T-cells. IFNG and GZMB were expressed in higher levels in MTBVAC while GZMM was slightly lower than in BCG-primed cells. In contrast, BCG-stimulated cultures showed a higher expression of genes related with type I IFN responses (e.g. ISG20, IFITM1). These findings indicate that activation of γδ T

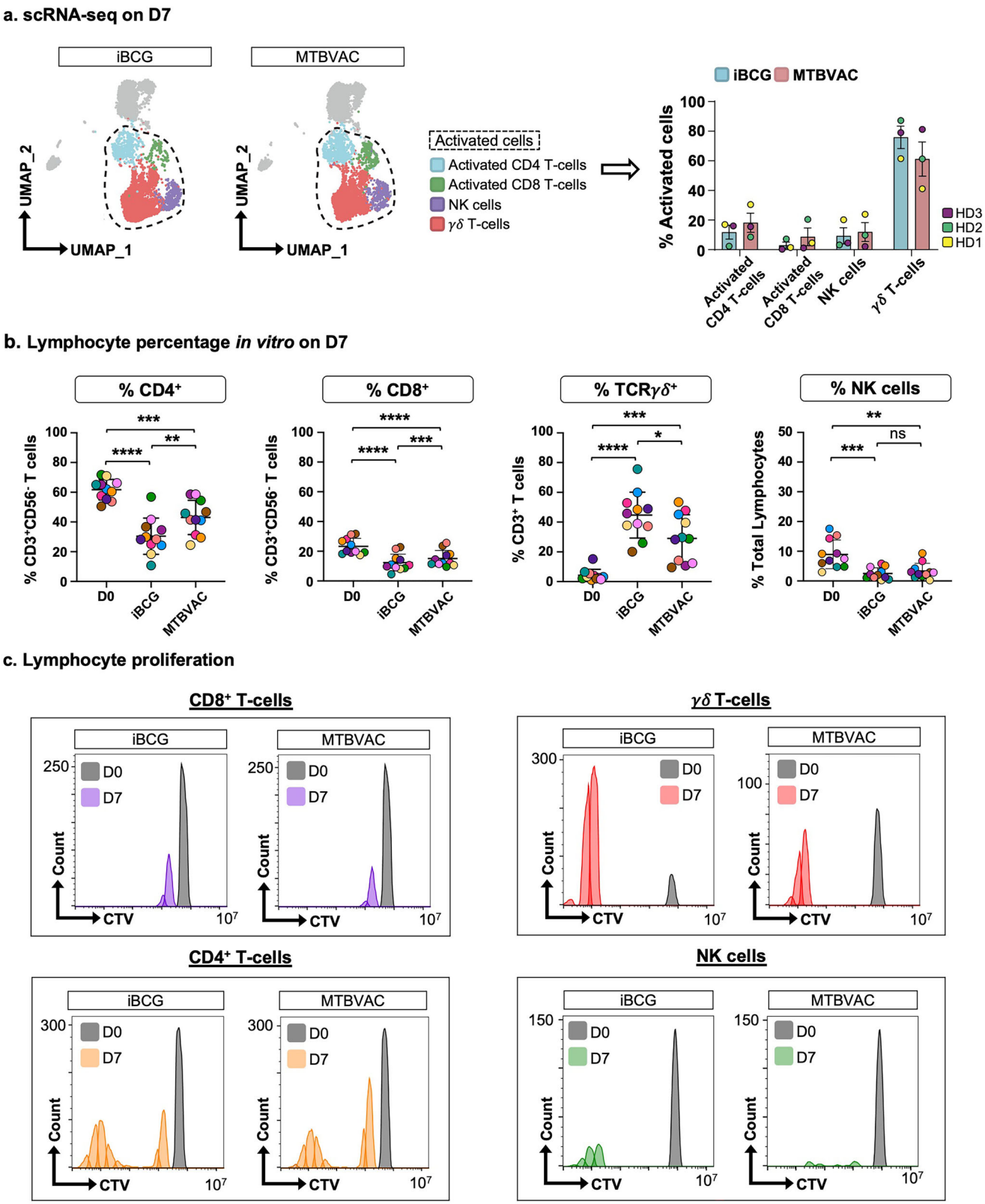

Fig. 1 | MTBVAC selectively enhances proliferation of CD4 and γδ T-cells. **a** PBMC clusters. PBMC from 3 healthy donors were incubated with either iBCG or MTBVAC for 7 days. scRNA-seq analysis allowed identification of 4 clusters of activated lymphocytes, highlighted in the UMAP plot (left). The frequency of these clusters within the total of iBCG or MTBVAC-activated cells is shown in bar plots (right); mean ± SD are depicted. Dots represent each healthy donor in a different colour. **b** Lymphocyte activation by FACS. PBMC from 11 healthy donors, depicted in different colours, were incubated with either iBCG or MTBVAC. After a week, cells were recovered, and the different subsets analysed by flow cytometry. Scatter plots show mean ± SD. Statistical analysis was done by paired sample t-test (*$p < 0.05$, **$p < 0.01$, ***$p < 0.001$, ****$p < 0.0001$) comparing % of activated cells with each vaccine against % on basal condition, D0, and between vaccines. **c** Activated lymphocytes proliferation. Profiles of lymphocyte subsets after one week of co-culture were analysed by flow cytometry. Data from a representative healthy donor are shown.

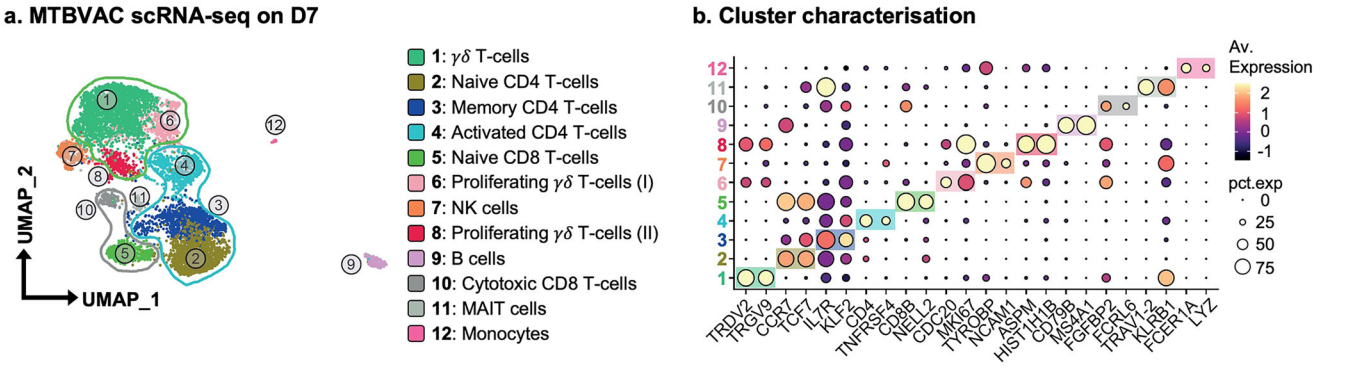

Fig. 2 | scRNA-seq analysis of MTBVAC-stimulated PBMC. a PBMC clusters. The MTBVAC-primed dataset from 3 healthy donors was analysed and clusters annotated using the FindClusters function from Seurat R package (see Materials and Methods). UMAP plot represents the 12 clusters identified. Selected clusters are grouped: CD4 (2, 3, 4), **blue line**; CD8 (5, 10), **grey line**; γδ T-cells (1, 6, 8), **green line**. **b** Cluster characterization. Dot plot represents average expression (colour graph) and % of cells (dot size) for markers (x-axis) defining each cluster (y-axis).

lymphocytes after stimulation with non-pathogenic mycobacteria can initiate a proinflammatory response and participate in homeostasis regulating infiltration of CD8 T-cells[27,28].

Since individuals from TB endemic regions that control the infection have an expanded population of $CD8^+$ γδ T-cells expressing the low affinity IgG receptor FcγRIII (CD16) that may help to control bacteria[18], we also evaluated these markers. FCGR3A was found in 21.2% of MTBVAC-primed γδ T-cells (Fig. 4e, f, Supplementary Fig. 6b), which is remarkable since, usually, this transcript is expressed at low levels in this subset. γδ T-cells expressing FCGR3A contained more markers of a cytotoxic profile, such as GNLY, GZMB, CX3CR1 (Fig. 4f). In contrast, iBCG priming resulted in a lower percentage of γδ T-cells expressing FCGR3A (14.4% in iBCG). Flow cytometry of γδ T-cells expanded after MTBVAC co-incubation confirmed that nearly 40% of γδ T-cells expressed significantly more CD16 (Fig. 4g) than those activated after BCG (20%). A small $CD8^+$ γδ T-cell population (mainly $CD8\alpha^+$) was also identified after incubating PBMC with either iBCG or MTBVAC vaccines (Supplementary Fig. 6c–e).

Besides expression of cytotoxic and proinflammatory molecules, the entire γδ T-cell population was activated, as cells had upregulated expression of CD25, HLA-DR and CXCR3 by flow cytometry (Fig. 4g). These γδ T-cells also expressed several NK receptors (Supplementary Fig. 4a), like NKG2D, but no PD1 expression was found (Fig. 4g). It is also intriguing that secondary lymphoid homing molecules have very different expression levels: while CD62L was increased in the whole γδ T-cell population, CCR7 was almost absent (Fig. 2b). Interestingly, in a bovine model, γδ T-cell skin egress and migration into lymph nodes was proposed to be mediated by CD62L expression, independently of CCR7[29].

In aggregate, a differentiated effector population loaded with cytolytic molecules, consistent with the $CD16^+GZMB^{hi}$ cytolytic γδ T-cells identified in individuals that controlled Mtb infection[18], was also found in MTBVAC-expanded PBMC. These cells can respond through antibody (via CD16) and NKG2D-mediated cytotoxicity and may have the capacity to home to secondary lymphoid organs. However, whether this population can be maintained over time after vaccination is as yet unknown.

After MTBVAC co-culture, NK and CD8 T-cell percentages decrease, but these populations are activated

In contrast to CD4 and γδ T-cells, the proportion of CD8 T lymphocytes and NK cells clearly decreased after MTBVAC stimulation of PBMC (Fig. 1c). Nevertheless, although the number of CD8 T-cells identified was low, an obvious cluster of cytotoxic CD8 T-cells (C10) could be distinguished from another of naïve CD8 T-cells (C5) (Fig. 2). High levels of GZMB and CCL4 defined the cytotoxic CD8 T cell cluster (Supplementary Fig. 7a) which also clearly expressed the transcription factors ZNF683, a marker of tissue resident memory, as well as ZEB2, the chemokine receptor CX3CR1, the integrin ITGB1 and the innate molecules KLRD1 and KLRG1, the latter associated with terminal differentiation of effector cells[30]. These cells were similar to the ones identified in iBCG cultures, but expressed more DDX5, further confirming an effector activation phenotype[31], and less ITGA4 (CD49d), present in virtual memory cells (Supplementary Fig. 7b). CD38 was also low in MTBVAC-primed cultures. Although expression of this marker usually occurs after T cell activation, a CD38/CD203/CD73 axis can also diminish T-cell functions[32,33]. In fact, other data indicate that low CD38 expression discriminates reprogrammable T-cells from $PD1^{hi}$ dysfunctional subsets[34]. So, MTBVAC-stimulated PBMC contain activated cytotoxic T-cells that are less likely to be exhausted.

Taken together, these data indicate that a small subset of non-exhausted effector CD8 T-cells can be clearly defined in cultures responding to MTBVAC stimulation.

Two subclusters of NK cells could also be identified in scRNA-seq, both with cytotoxic features and expressing molecules consistent with a $CD56^{dim}$ phenotype (Fig. 5a, b). However, SC2, expressing both IL2RA and IFNG (Supplementary Fig. 7c), represents a more active subset than SC1. SC2 also expressed FASLG, TNFRSF18, CSF1 and IL21R, and so are NK cells with great potential to kill target cells (Fig. 5c). Comparison between MTBVAC and BCG-primed NK cells revealed only small differences (Fig. 5d). Notably, although GZMB was strongly transcribed in NK cells from both cultures, its expression was even stronger after MTBVAC-stimulation. Taken together, these features of NK cells indicate that they might potently kill target cells.

Functional capacities of MTBVAC-stimulated cultures

The range of cytokines produced by PBMC, after a 7-day co-culture with MTBVAC, were studied by analysing mRNA transcripts in the different cell populations identified in scRNA-seq, and these experiments were complemented by Luminex analyses of a panel of effector and suppressor cytokines secreted into tissue culture supernatants of MTBVAC- and iBCG-stimulated PBMC (Fig. 6).

Consistent with the observation that MTBVAC stimulation led to expansion of mainly IFN-γ-producing lymphocyte populations, the presence of this cytokine was clearly detected in supernatants, while IL-2 and IL-4 were almost undetectable. TNF-α and IL-6 were also produced by MTBVAC-activated PBMC (Fig. 6a), while IL-17A and IL-17F were only detected in extremely low concentrations. These data confirmed the scRNA-seq analyses, in which the secretion of each cytokine can be associated to the producing cell subcluster (Supplementary Fig. 8a). Feature-plots of the cytokines secreted by activated CD4 T-cells, revealed high levels of IFNG, CSF2 (GM-CSF) and IL26 transcription (Fig. 3d). Interestingly, IL26 has been described to have anti-microbial function and bind mycobacteria derived lipoarabinomannan (LAM)[35]. On the other hand, TNF and IL21 were only expressed in low amounts by CD4 cells and IL17A was virtually absent. As mentioned before, γδ T-cells also transcribed high levels of IFNG, TNF and IL15 (Supplementary Fig. 8b).

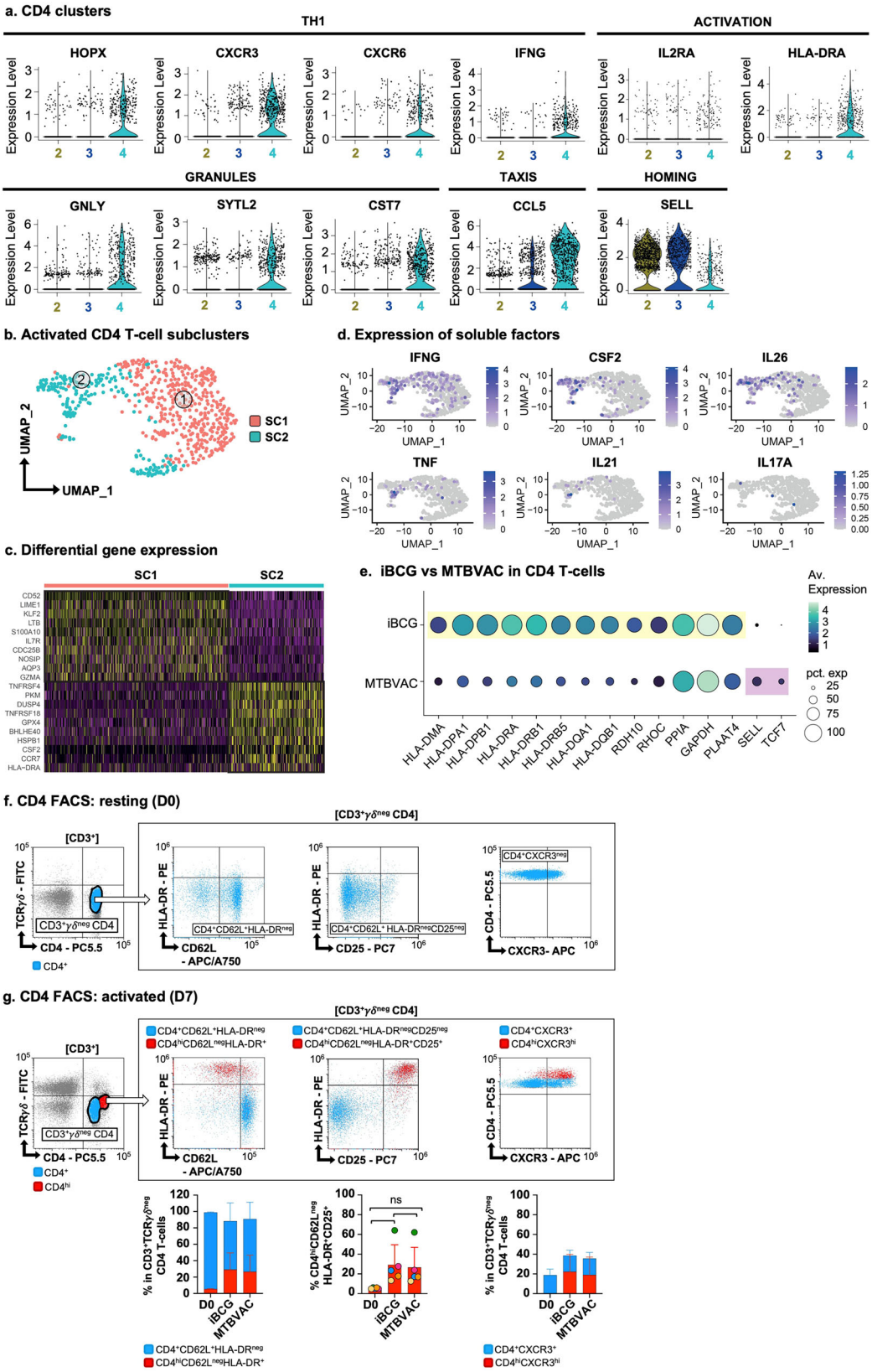

Taken together these data confirm the secretion of cytokines expected from a majority Th1 CD4 T-cell population, such as IFN-γ and TNF-α. However, the concentration of these factors was enhanced by the contribution of a specialized effector γδ T-cell population.

BCG has been used for decades as therapeutic agent against bladder cancer and NK cells activated with BCG are very efficient killing tumours via NKG2D[36]. Therefore, it was of interest to test whether MTBVAC could have some role as a cancer therapeutic. We confirmed that MTBVAC-primed

Fig. 3 | Characterisation of MTBVAC-stimulated CD4 T-cells. a Violin plots. Violin plots show expression level of signature markers for the CD4 clusters (2, 3, 4) (x-axis) identified in Fig. 2. **b–d** Activated CD4 T-cell analysis. UMAP plot of cluster 4 from Fig. 2 (**b**) identified two subclusters (SC1, SC2). The 10 most differentially expressed genes of SC1 and SC2 are shown in a heatmap (**c**). Feature plots highlight the expression of IFNG, CSF2, IL26, TNF, IL21 and IL17A within activated CD4 T-cells (**d**). **e** CD4 T-cell differences after exposure to vaccines. iBCG and MTBVAC-stimulated CD4 T-cells were analysed by differential marker expression (x-axis) in a dot plot. The average expression level and percentage of cells expressing a particular marker is shown using colour density and dot size respectively. **f**, **g** Activation markers by FACS. Representative plots show HLA-DR, CD62L, CD25 and CXCR3 markers within $CD3^+$ $TCR\gamma\delta^{neg}$ CD4 T-cells from PBMC on D0 (**f**) and on PBMC one week after incubation with MTBVAC (**g**). Gating strategies are shown for both resting and activated states. For activated PBMC (**g**), the frequency of selected populations is plotted in either bar graphs or scatter plots ($n = 5$; mean ± SD). For the $CD4^{hi}$ $CD62L^{neg}$ $HLA\text{-}DR^+$ $CD25^+$ subpopulation, a scatter plot shows the frequency against basal state, D0, and between vaccines compared by a by paired sample t-test (ns: $p > 0.05$) for the 5 healthy donors, depicted in different colours.

NK cells increased NKG2D cell surface expression (Supplementary Fig. 9a). Killing assays using MTBVAC-primed PBMC, as effectors, against several bladder cancer cell lines as target cells (Supplementary Fig. 9b–d) revealed that, although the levels of tumour target lysis were in general low, they could be related to the percentage of NK cells present in the cultures at day 7. Degranulation experiments showed that NK cells (Fig. 7a), and to a lesser extent γδ T-cells (Supplementary Fig. 10a), were the main subpopulation degranulating against K562 control target cells. However, degranulation was generally weak against bladder cell lines. On the other hand, intracellular staining at day 7 showed that NK cells released low or no IFN-γ and TNF-α after recognition of K562 and bladder cancer cells (Fig. 7b, c; Supplementary Fig. 10b, c). These experiments indicate that BCG stimulates anti-tumour NK cells slightly more efficiently than MTBVAC.

Discussion

To date, there is limited characterization of human cellular immunity generated in response to MTBVAC while more detailed immune profiling has been done in animal models. This paper presents in-depth evaluation of the lymphocyte subpopulations stimulated early after stimulation with the new live-attenuated MTBVAC vaccine, demonstrating that a particular effector and memory response is generated. Comparison with BCG was done to unveil any molecular differences that could allow each vaccine to affect certain aspects of the various pathogenic manifestations of Mtb infection. To address this, we analysed the phenotype of PBMC 7 days after co-incubation with either MTBVAC or iBCG. The results demonstrate that, although CD4 T-cells and γδ T-cells proliferate after leukocyte activation with BCG and MTBVAC, the phenotypic and functional features of these cells can be very different. Innate cells from MTBVAC cultures, in particular γδ T-cells, display a phenotype consistent with that found in young donors controlling Mtb infection in endemic countries, that is, $CD16^+GZMB^+$ effectors. The expression of GZMB, along with other maturation and activation markers such as GNLY, HAVCR2 (TIM3), IL2RA, TNFRSF9 (4-1BB), and the entire set of secreted cytokines (IFNG, TNF, CSF2, IL15, etc.) suggests that these γδ T-cells, while still maintaining CD27 expression, are sufficiently activated to give rise to a functional and effector response.

This in vitro study provides important insights into the acute immune response generated by exposure of human peripheral blood to MTBVAC. The most interesting findings are those related to the proliferating innate lymphocytes, mainly γδ T-cells and NK cells, together with the substantial CD4 T-cell response.

Focussing first on innate responses, previous studies in TB patients have shown that innate immune cells change during progression to disease and clearance. Roy Chowdhury et al.[18] studied, in a highly endemic area, a cohort with low rate of active TB in young children and adults, indicating that these individuals could control Mtb infection. Although a spectrum between donors with complete bacterial clearance and other donors with active control of subclinical disease could have been included in that study, the data clearly identify a CD8+ γδ T-cell subset with attenuated TCR mediated responses, but expressing CD16. The presence of CD16, a low affinity receptor of IgG, allows γδ T-cells to mediate antibody-dependent cellular cytotoxicity (ADCC)[18]. In this population, a reduced frequency of NK cells was also associated with active disease[15]. Vγ9Vδ2 T-cells have previously been described to expand in the PBMC of BCG-vaccinated individuals, after secondary stimulation with Mtb lysates[37]. Here we show that the active population of MTBVAC-stimulated γδ T-cells have considerable cytotoxic potential, as shown by the high expression of granzymes and granulolysin, with a proinflammatory $CD27^+$ IFN-γ^+ phenotype and with the possibility to have a stronger capacity to perform ADCC, from the greater upregulation of $CD16^+$ than BCG stimulated cells. Importantly, the single cell resolution transcriptomics and flow cytometry data were very consistent, strongly supporting all conclusions. Initially, the finding of CD16 on γδ T-cells was surprising. However, CD16 upregulation has been previously described, in other contexts. For example, $CD16^+$ activated γδ T-cells were also described after stimulation with bacterial pyrophosphate antigens and cytokines[38]. Other $CD16^+$ γδ T-cells were from $V\delta1^+$ and $V\delta3^+$ subsets[39], but the γδ T-cells expanded in cultures described here are mainly $V\delta2^+$. In patients clearing Mtb[18], $CD8^+CD16^+$ cytotoxic γδ T-cells, had effector-memory features, with low expression of CCR7, CD27, CD28, CD62L, and CD127 and preferential expression of certain NK receptors, compared with the CD8 negative subset. Many of these markers were also found in MTBVAC-primed γδ T-cells, suggesting that the use of an Mtb-based vaccine can activate immune responses that could help to control infection better than *M. bovis*-based vaccines. However, it would be of great interest to evaluate the presence of this population in vaccinated individuals and how persistent they are in time. In this context, it is interesting to note that the $CD8^+$ γδ T-cells described by Chowdhury et al. are increased in a range of chronic or persistent inflammatory conditions, suggesting that the degree of antigen persistence and chronic stimulation may be key factors influencing the induction of distinct γδ T-cell effector programs. Additionally, it has also been reported that cytokine receptor pathways and Jak/Stat signalling are upregulated in Mtb infected macrophages, whereas M. bovis infection leads to enhanced macrophage apoptosis[40]. Thus, we speculate that differences in macrophage cytokine release after MTBVAC or BCG infection might also influence subsequent γδ T-cell expansion and differentiation. This hypothesis is consistent with our observation that MTBVAC-primed cultures released pro-inflammatory cytokines corresponding to effector phenotypes.

Initially, a panel of cytokines designed to detect factors released in the context of CD4 activation, suggested a Th1 versus regulatory response. However, this panel did not enquire on cytokines sharing the gamma chain with IL-2, like IL-15 and IL-21. scRNA-seq demonstrated strong transcription of IL-15, but not IL-21. Detection of high concentrations of TNF-α and IFN-γ, again suggest activation of effector lymphocytes and is consistent with previous data demonstrating that Vγ9/Vδ2 T-cells expanded with IL-15 secrete TNF-α and IFN-γ, and that IL-21 impaired this secretion. Regarding regulatory suppressor aspects, the lack of IL-17A in MTBVAC cultures illustrates another advantage of using a non-pathogenic Mtb-derived vaccine. In mice, TB infection leads to IL-17 production in lung[41] and, in patients with active pulmonary disease, IL-17 is produced by peripheral blood γδ T-cells[19]. It has been suggested that an IL-17 increase in disease, promoted by antigen and IL-1β, IL-6, IL-23, and TGF-β[42], could be responsible for the formation of granulomas in pulmonary TB. Cytokines regulate immune cell activation, proliferation, and cytotoxic function. So, it seems likely that the cytokine and granule protein differences identified would be linked. Many cytokines, such as IL-2, IL-15, and IFN-γ, enhance the expression and release of granule proteins like perforin and granzymes, which are crucial for target cell killing. Although IL-2, IL-15 and IL21 share the common cytokine-receptor γ-chain (γc), in adaptive responses they can

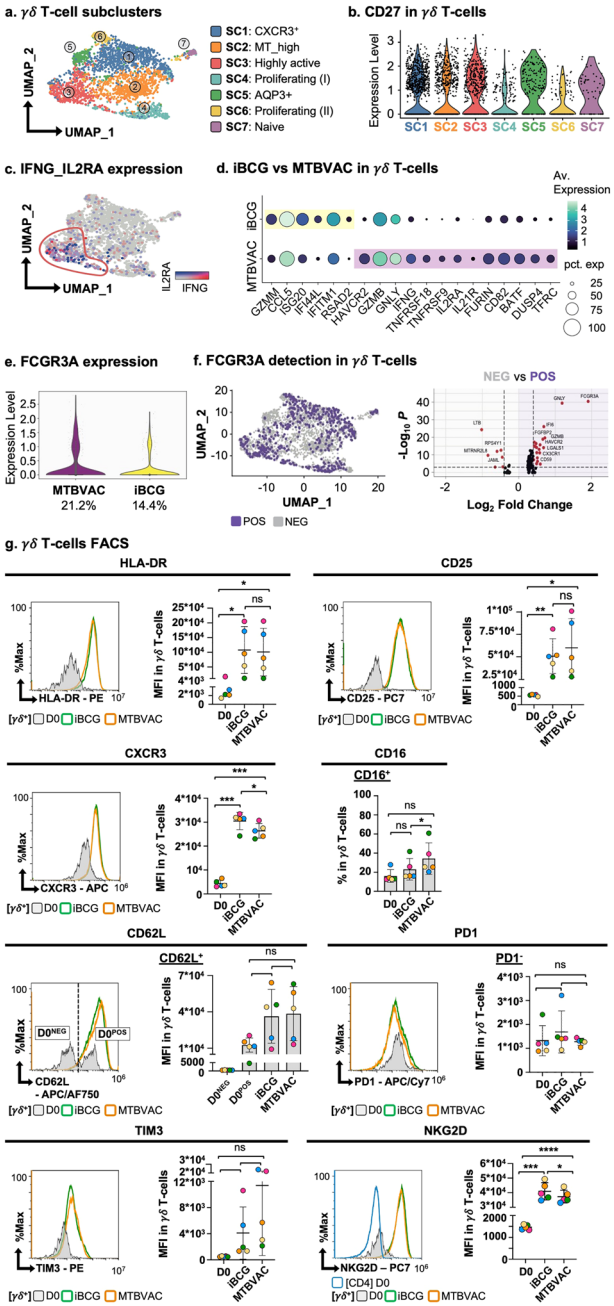

Fig. 4 | Characterisation of MTBVAC-stimulated γδ T-cells. a–f scRNA-seq. **a** UMAP plot represents γδ T-cell subclusters from the 3 healthy donors of Fig. 2. **b** Violin plot showing expression of CD27 for each γδ T-cell subcluster. **c** Feature plot of IFNG and IL2RA markers in γδ T-cells. **d** Dot plot of markers (x-axis) discriminating γδ T-cells from iBCG and MTBVAC experiments. The average expression level and percentage of cells expressing a particular marker are shown using colour density and dot size respectively. **e** Violin plots comparing the expression of FCGR3A in γδ T-cells from MTBVAC and iBCG cultures. **f** FCGR3A expression in γδ T-cells from MTBVAC cultures: UMAP highlighting γδ T-cells with positive values of FCGR3A (left) and volcano plot of differentially expressed genes between γδ T-cells expressing (POS) or not expressing (NEG) FCGR3A (right). Genes with a Log2FC > 0.58 and a Bonferroni adjusted *p*-value < 0.05 are marked in **red**. **g** γδ T-cell phenotype by FACS. PBMC from 5 healthy donors were incubated with either iBCG or MTBVAC for a week and cells were analysed by flow cytometry. For each marker, representative histograms and MFI scatter plots (mean ± SD), with each donor represented in different colour, are shown. Statistical analysis of % of expression against expression on basal condition, D0, and between vaccines was done by paired sample t-test (*$p < 0.05$, **$p < 0.01$, ***$p < 0.001$, ****$p < 0.0001$).

have competing activities[43,44]. The panel of cytokines measured by Luminex in PBMC cultures stimulated with MTBVAC, included only factors released in the context of CD4 activation, to distinguish Th1 from regulatory events. Thus, the only member of the common gamma chain family tested was IL-2, which was found in low levels. RNA-seq revealed that IL15 transcript was present in γδ T-cells. This would suggest an enhanced response of innate vs regulatory lymphocytes, and particularly the potentiation of cytotoxic capacity[45–47] and proliferation[48,49]. Indeed, the phenotype of cells harvested 7 days after stimulation correspond to cytotoxic cells with a high proportion of innate immune lymphocytes.

About the genes differentially expressed in γδ T-cells, both HAVCR2 (TIM3) and TNFRSF9 (4-1BB) have been associated with T cell activation, inhibition or exhaustion in different contexts[24,26,50]. For example, in Mtb infection TIM3 could mediate activation against galectin-9-expressing macrophages[51]. Thus, further studies are needed to determine its role in the context of vaccination. Moreover, analysing peripheral blood of vaccinated individuals (BCG and MTBVAC) could shed light on the roles of specialized γδ T-cell populations in Mtb control.

The other major population expanded in MTBVAC co-cultures is a Th1-like CD4 T-cell population, secreting IFN-γ, CSF2, IL-26 and TNF-α and expressing CXCR3. The main difference in $CD4^+$ T-cell responses elicited by the two vaccines, iBCG and MTBVAC, was the higher expression of MHC class II genes after co-culture with iBCG and the transcription of SELL (CD62L) in MTBVAC-stimulated cells. RNA expression of HLA-DRB1 by non-naïve CD4 T-cells is increased in patients with active TB at diagnosis, before the start of anti-TB therapy. HLA-DR has been suggested to indicate cells that divided after antigen encounter[52]. In flow cytometry, HLA-DR positive cells were clearly activated ($CD25^+$ $CD62L^{neg}$), while $CD62L^+$ lymphocytes expressed neither CD25 nor HLA-DR. Since this is a dynamic process that we have studied at a single time point, it is difficult to know whether this would imply earlier or simply a differential pattern of activation. In any case, a higher activation profile of CD4 T-cells (DR^+ $CD25^+$ $CD62L^{neg}$) by MTBVAC compared to BCG cultures was detected. It is tempting to speculate that, besides the activation profile of CD4 and CD8 T-cells, γδ T-cell activation by these vaccines could also enhance the generation of tissue-resident memory lymphocytes, as reported in murine models[27]. In fact, the observation of populations of CD4 T-cells with low expression of KLF2 and SIPR1 and higher levels of ITGAE (CD103) would be consistent with this idea. Likewise, enhanced expression of ZNF683 (Hobit), found in CD8 T-cells, is another indicator of tissue resident memory lymphocytes (Supplementary Fig. 11).

As is seen for BCG, culture of PBMC with MTBVAC yielded cytotoxic effector NK cells, however the functional data indicate that MTBVAC-stimulated NK cells showed clear degranulation against a very good NK target, the K562 cell line, and were less reactive against bladder cancer cells. However, clear cytotoxicity of tumour cells was elicited by PBMC. This fact, together with data in murine models, where MTBVAC was able to eliminate bladder cancer in conditions in which BCG did not work[53], implies that other mechanisms could be involved in recognition of tumours by MTBVAC-primed cells.

Altogether, MTBVAC stimulates an effective early immune response from the first week of interaction with PBMC with the generation of effector lymphocyte populations including CD4 and γδ T-cells, with phenotypes consistent with those observed in individuals that can control mycobacterial infections and populations of tissue resident memory.

Finally, this study presents potential limitations: comparison of early activation of PBMC using either MTBVAC and BCG was performed, a dynamic process that could imply transient activation of certain immune populations. Thus, analysis at other time points between day 0 and 7 would be informative. Also, all the experiments were done in vitro, using healthy donor PBMC and not drawing blood from vaccinated individuals. To strongly conclude that MTBVAC elicits a particular, beneficial innate population activation, identification of these subsets should be studied in vaccinated donors and related to TB protection.

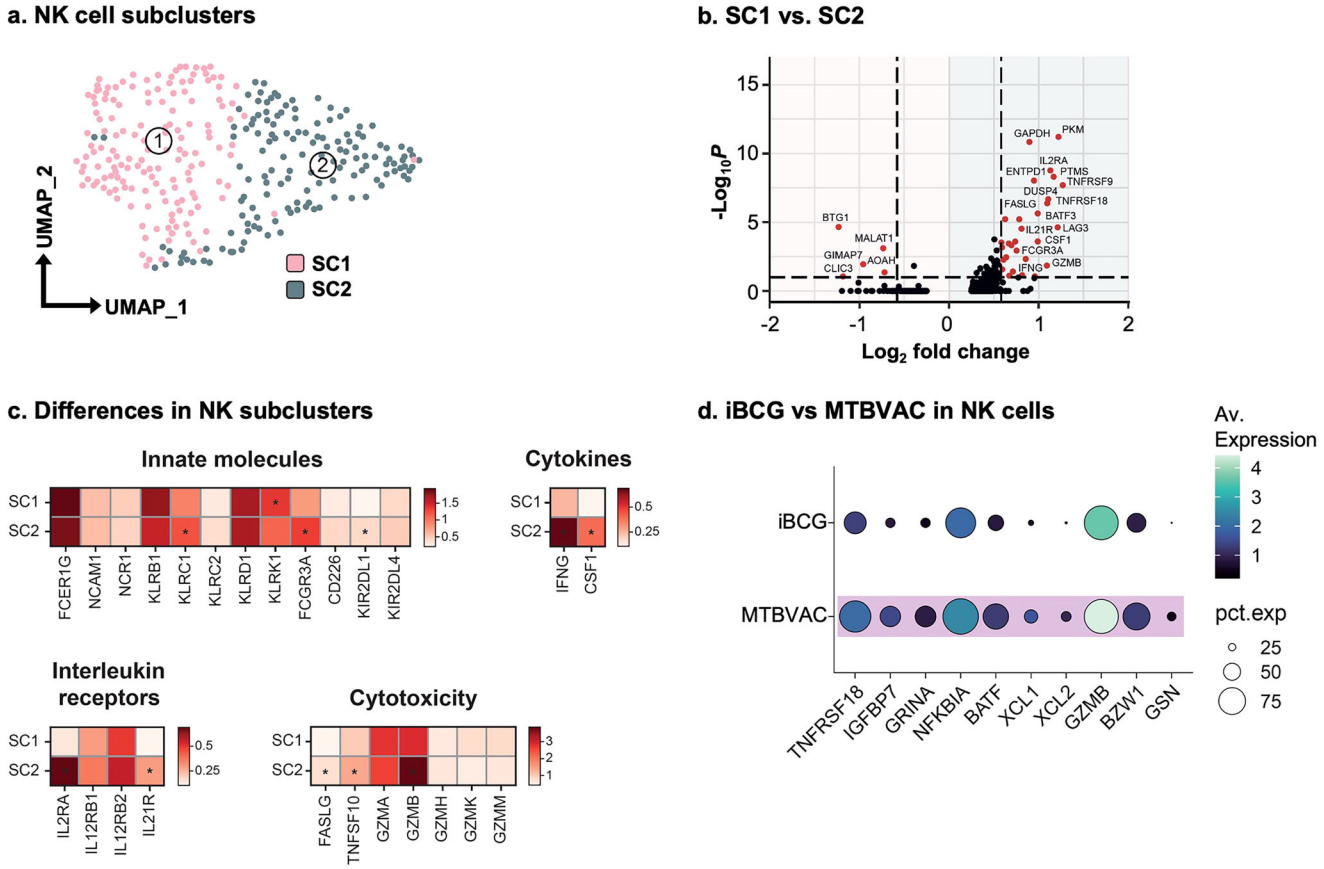

Fig. 5 | Characterisation of MTBVAC-stimulated NK cells by scRNA-seq. Analysis of NK cell subpopulations from MTBVAC-primed PBMC identified in 3 healthy donors in Fig. 2. **a** UMAP. Plot shows two NK cell subclusters (SC1, SC2). **b** Volcano plot. Genes differentially expressed between NK cell subclusters SC1 and SC2 are highlighted, marking in **red** genes with a Log2FC > 0.58 and a Bonferroni adjusted *p*-value < 0.05. **c** Matrix plot. Expression of markers within each NK cell subcluster are indicated according to colour scale. Markers differentially detected between both subclusters are highlighted with an asterisk. **d** Dot plot. Different markers (x-axis) in NK cells from iBCG and MTBVAC experiments. The average expression level and percentage of cells expressing a particular marker are shown using colour density and dot size respectively.

Materials and methods

BCG and peripheral blood

PBMC from buffy coats of healthy donors were obtained from the Regional Transfusion Centre, Madrid, with informed consent from the participants and with the ethical permission and experimental protocols approved by local and CSIC bioethics committees. All methods were carried out in accordance with biosafety guidelines and regulations authorized by CNB-CSIC.

PBMC were isolated by centrifugation on Ficoll-HyPaque and cultured in complete (2 mM L-glutamine, 0.1 mM nonessential amino acids, 1 mM sodium pyruvate, 100 U/mL penicillin, 100 U/mL streptomycin, 10 mM Hepes, 50 μM β-mercaptoethanol) RPMI-1640 medium (Biowest) supplemented with 5% FBS (Capricorn), 5% HS (Sigma).

BCG-Moreau RJ strain (ImunoBCG, iBCG) and MTBVAC vials were from Biofabri, Spain. Aliquots with a viability of 2.3% and 11.3%, respectively, were reconstituted in complete RPMI-1640 medium 10% DMSO and stored at −80 °C.

BCG-mediated stimulation

PBMC co-culture with BCG in vitro model was described previously[22,36,54]. Briefly, 10^6 PBMC/ml were incubated in 24-well plates with or without mycobacteria at a 6:1 ratio (total bacteria to PBMC). After one week in culture, cells in suspension and supernatants were recovered for analysis.

Flow cytometry

Cells were washed with PBA [PBS supplemented with 0.5% bovine serum albumin (BSA), 1% FBS and 0.065% sodium azide] and incubated with antibodies against surface markers: CD3-PB, CD16-PE/Cy7, CD4-PC5.5, CD8-APC/Cy7, CD25-PE/Cy7, L-selectin (CD62L)-APC Fire™ 750; LAMP1 (CD107a)-APC; CD138 (CXCR3)-APC; CD279 (PD1)-APC/Cy7; TCRγδ-FITC; CD314 (NKG2D)-PE/Cy7; CD366 (TIM3)-PE; HLA-DR-PE (Biolegend); CD56-PC5 (Beckman Coulter). For extracellular staining, cells were directly incubated with the appropriate conjugated antibodies at 4 °C for 30 min in the dark. For intracellular staining, after surface labelling, cells were fixed with 1% p-formaldehyde for 10 min at RT, permeabilized with 0.1% saponin for 10 min at RT. After staining, cells were washed in PBA and analysed using CytoFLEX S flow cytometer (Beckman Coulter). Analysis of the experiments was performed using Kaluza software.

scRNA-seq

Sample preparation, library generation, sequencing and data analysis have been previously described[22]. Library pools from MTBVAC-stimulated PBMC were sequenced at 650 pM in paired-end reads on a P3 flow cell using NextSeq 2000 (Illumina) at the Genomics Unit of the Centro Nacional de Investigaciones Cardiovasculares (CNIC, Madrid).

Cell Ranger (v6.0.2) count was utilized for the alignment and quantification of raw gene expression data sourced from GEX and HTO FASTQ files. After that, cells were filtered to retain only high-quality singlets by removing those with fewer than 200 or more than 5000 features, as well as those with a mitochondrial content exceeding 10%. Oligo-tagged antibodies were employed to identify and eliminate doublets, with hashtag counts normalized using Centered Log-Ratio transformation and demultiplexed through the HTODemux pipeline.

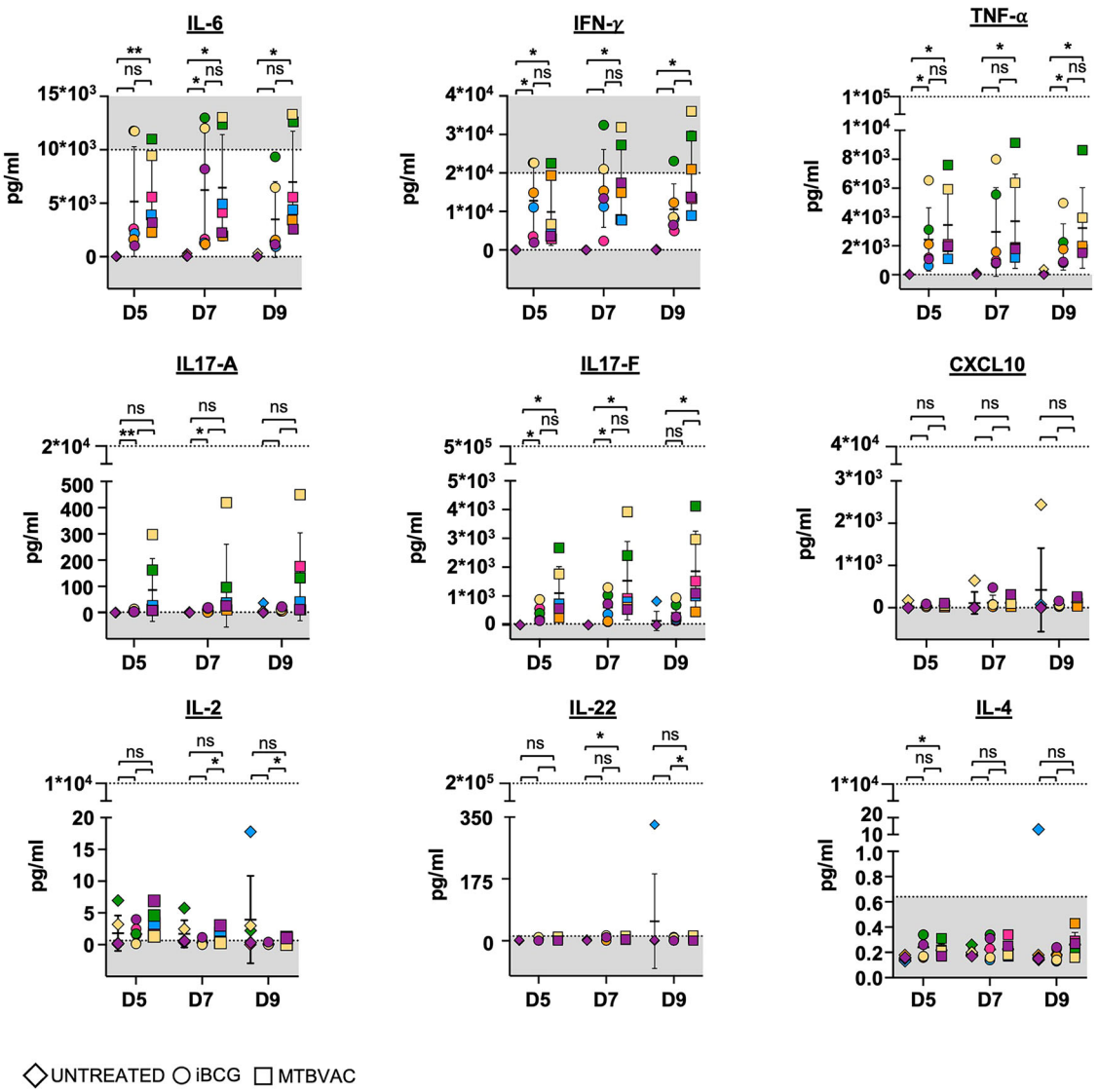

Fig. 6 | Cytokine profile after 7-day exposure to vaccines. PBMC from 6 healthy donors (depicted in different colours) were incubated with either iBCG (◯) or MTBVAC (□). After 5, 7 and 9 days in culture, cell supernatants were recovered for cytokine quantification by Luminex. Scatter plots show mean ± SD for each condition. Limits of detection are indicated in grey. Statistical analysis of cytokine concentration in activated cultures compared to the untreated condition (◇) and between vaccines on the same day was done by paired sample t-test (*$p < 0.05$, **$p < 0.01$, ***$p < 0.001$, ****$p < 0.0001$).

The primary R package utilized for data manipulation and visualization was Seurat (v4.0.2). Seurat objects were individually analysed or, otherwise, integrated, and gene expression (GEX) counts were normalized and log-transformed. Principal component analysis (PCA) was carried out on variable features, and the initial N principal components, determined using the ElbowPlot method, were employed for Shared Nearest Neighbor (SNN) clustering and UMAP visualization.

Cell clustering was conducted at a resolution of 0.5, and the FindMarkers function was used to investigate cluster-specific characteristics and conduct overall annotation. To explore differences between clusters, functions such as DotPlot, ViolinPlot, FeaturePlot and DoHeatmap from the Seurat R package were utilized, along with the matrixplot function from the Scanpy (v1.9.1) Python toolkit.

Proliferation assays

PBMC were incubated with 2 µM CellTrace™ Violet stain (Invitrogen) for 20 min at 37 °C 5% CO_2. Complete RPMI-1640 medium (Biowest) 5% FBS (Capricorn), 5% HS (Sigma) was then added for 5 min and the cells were washed once with complete medium before plating in 24-well plates in the presence of either vaccine. After seven days in culture, cells were recovered and analysed by flow cytometry.

Cytokine release and intracellular staining

After co-culture of PBMC with vaccine, tissue culture supernatants were recovered, centrifuged at 200 × *g* to eliminate cells and stored at −80 °C until Luminex analysis. Samples were analysed using magnetic Luminex ® screening assays (R&D Systems) and Luminex®100™ (Qiagen) Luminex analyser instrument, according to manufacturer's instructions. Five-parameter logistic standard curves were generated and concentration within each sample were interpolated (considering the dilution factor) using the Bio-Plex Manager™ Software (Bio-Rad). Limits of detection (in pg/ml) for each measured cytokine (lower – upper) were considered as follows: IFN-γ (1.28 – 20 000); IL2 (0.64 – 10 000); IL4 (0.64 – 10 000); IL6 (0.64 – 10 000); IL17A (1.28 – 20 000); IL17F (32 – 500 000); IL22 (12.8 – 200 000); CXCL10 (2.56 – 40 000); TNFα (6.4 – 100 000).

For intracellular cytokine staining, PBMC were co-cultured with target cells for 6 h at 1:2 E:T ratio at 37 °C, 5% CO_2. After 1 h of co-incubation, brefeldin-A (Biolegend) was added to a final concentration of 5 µg/ml. 5 h

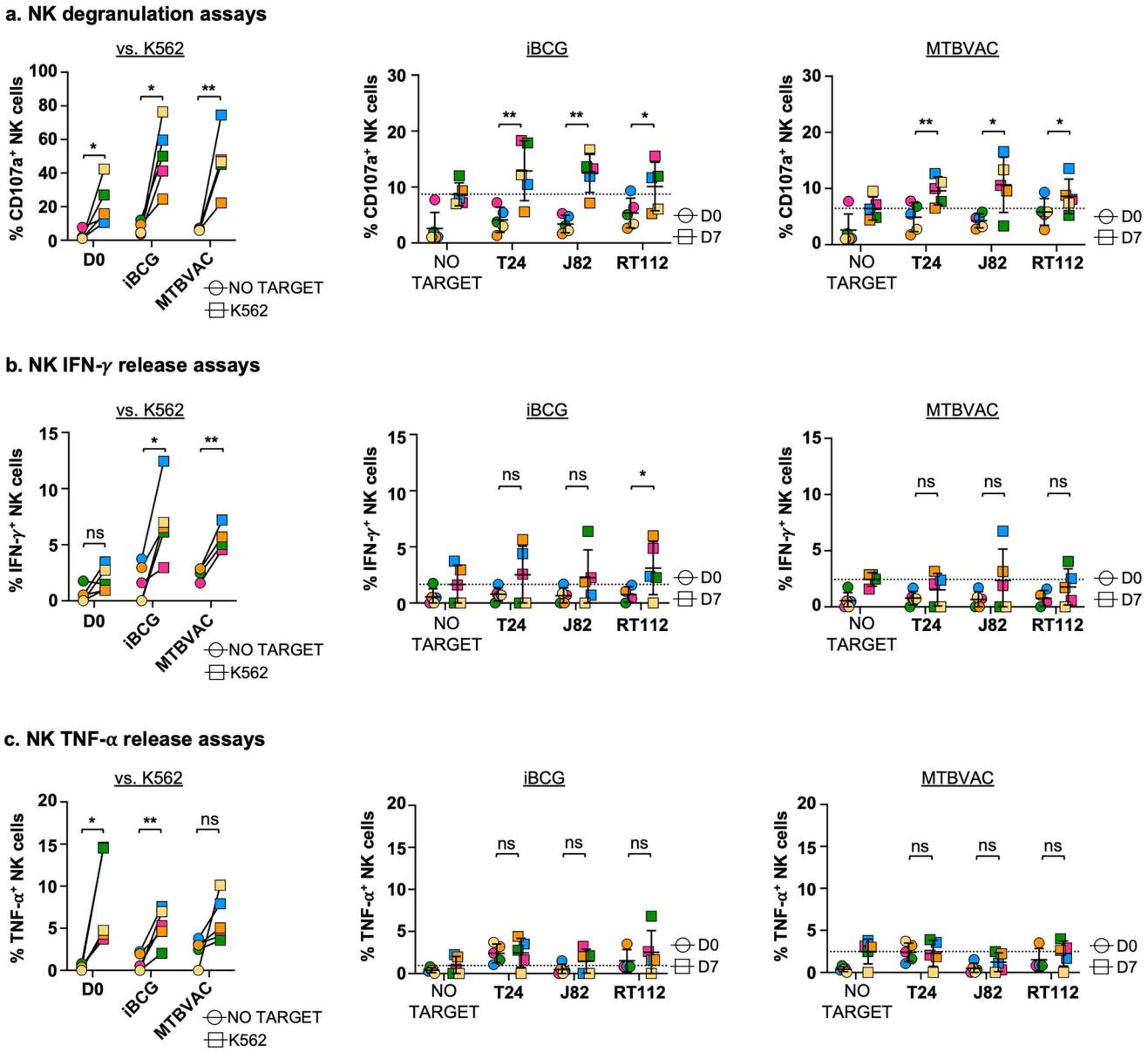

Fig. 7 | Effector function of stimulated lymphocytes against bladder cancer targets. PBMC from 5 healthy donors were incubated with iBCG or MTBVAC. After a week in culture, cells were recovered and used as effector cells against solid tumour bladder cancer cells: T24, J82, and RT112 or the positive control NK cell target K562, as indicated. **a** Degranulation. Activated PBMC were tested as effector cells (1:2 E:T ratio) and degranulation measured as surface LAMP-1 (CD107a). Scatter plots show mean ± SD for $n = 5$ (each healthy donor represented in a different colour). **b**, **c** Intracellular IFN-γ and TNF-α production by FACS. Dot line shows mean value on D7 against no target. Statistical analysis compared to basal expression on D0, was done by paired sample t-test (*$p < 0.05$, **$p < 0.01$, ***$p < 0.001$, ****$p < 0.0001$).

later, cells were recovered, fixed, permeabilised, and stained using using anti-IFNγ-APC/Cy7 and anti-TNFα-APC (Biolegend) for FACS analysis.

Degranulation experiments

PBMC from healthy donors were used as effector cells. Bladder cancer cell lines T24, J82, and RT-112 (ATCC) were used as target cells. K562 cells were used as positive control. 25000 effector were incubated with 50000 target cells (1:2 E:T ratio), for 2 h as described[55]. Surface expression of LAMP1 (CD107a) was analysed by flow cytometry.

Cytotoxicity assays

Bladder cancer cell lines T24, J82, and RT-112 (ATCC) were used as target cells. 10^4 target cells were plated in 96-well flat-bottom plates in triplicates in a final volume of 0.2 mL and let to adhere overnight. The next day, cells were labelled for 1 h with medium containing 3 µM calcein-AM (Invitrogen), washed 3 times and incubated in fresh medium for a further hour to release free dye. Cells were resuspended in complete RPMI-1640 without phenol red (Gibco) to minimise interference. PBMC were used as effector cells and incubated with adherent target cells for 3 h at 37 °C and 5% CO_2 at a 30:1 E:T ratio. Supernatants were recovered, after centrifugation at 270 × *g* for 5 min to pellet cells and transferred to a clean opaque plate (clear bottom). Calcein-AM release was determined by measuring absorbance (excitation wave 485 nm and emission wave 535 nm), using BioNova® F5 System. Specific lysis was calculated as the ratio [(value − spontaneous release)/(maximum release− spontaneous release)] × 100. Spontaneous release corresponds to labelled target cells without effector cells. Maximum release was determined by lysing the target cells in 0.5% Triton X-100 (Invitrogen). In all the experiments, the spontaneous release was between 20% and 30% of the maximum release.

Statistical analysis

Graphpad Prism 9 software was used for statistical analysis and representation of the data. Results were generally presented either as

individual values or as the mean and standard deviation (SD) (mean ± SD), as indicated in the text of in the figure legends. Statistically significant differences were evaluated with paired parametric t-tests according to the following criteria: $^{*}p < 0.05$, $^{**}p < 0.01$, $^{***}p < 0.001$, $^{****}p < 0.001$. When $p > 0.05$, differences were considered not significant and, therefore, are not indicated.

Data availability

R code related to the main scRNA-seq figures can be found at GitHub (https://github.com/algarji/Felgueres_MTBVAC). scRNA-seq data from MTBVAC stimulated PBMC are deposited at Gene Expression Omnibus (GEO) under the accession code GSE268279. Published scRNA-seq data from iBCG stimulated PBMC are available at GEO under the accession code GSE203098.

Received: 20 September 2024; Accepted: 14 March 2025;
Published online: 28 March 2025

References

1. Chakaya, J. et al. The WHO Global Tuberculosis 2021 Report – not so good news and turning the tide back to End TB. *Int. J. Infect. Dis.* **124**, S26–S29 (2022).
2. Lange, C. et al. 100 years of Mycobacterium bovis bacille Calmette-Guerin. *Lancet Infect. Dis.* **22**, e2–e12 (2022).
3. Mangtani, P. et al. Protection by BCG vaccine against tuberculosis: a systematic review of randomized controlled trials. *Clin. Infect. Dis.* **58**, 470–480 (2014).
4. Andersen, P. & Doherty, T. M. The success and failure of BCG — implications for a novel tuberculosis vaccine. *Nat. Rev. Microbiol.* **3**, 656–662 (2005).
5. Kaufmann, S. H. E. Vaccine Development Against Tuberculosis Over the Last 140 Years: Failure as Part of Success. *Front. Microbiol* **12**, 750124 (2021).
6. Gandhi, N. M., Morales, A. & Lamm, D. L. Bacillus Calmette-Guerin immunotherapy for genitourinary cancer. *BJU Int.* **112**, 288–297 (2013).
7. Arbues, A. et al. Construction, characterization and preclinical evaluation of MTBVAC, the first live-attenuated M. tuberculosis-based vaccine to enter clinical trials. *Vaccine* **31**, 4867–4873 (2013).
8. Tameris, M. et al. Live-attenuated Mycobacterium tuberculosis vaccine MTBVAC versus BCG in adults and neonates: a randomised controlled, double-blind dose-escalation trial. *Lancet Respir. Med.* **7**, 757–770 (2019).
9. Spertini, F. et al. Safety of human immunisation with a live-attenuated Mycobacterium tuberculosis vaccine: a randomised, double-blind, controlled phase I trial. *Lancet Respir. Med.* **3**, 953–962 (2015).
10. Moreo, E. et al. Novel intravesical bacterial immunotherapy induces rejection of BCG-unresponsive established bladder tumors. *J. Immunother. Cancer* **10** (2022).
11. Drain, P. K. et al. Incipient and Subclinical Tuberculosis: a Clinical Review of Early Stages and Progression of Infection. *Clin. Microbiol. Rev.* **31**, https://doi.org/10.1128/cmr.00021-00018 (2018).
12. Flynn, J. L. & Chan, J. Immune cell interactions in tuberculosis. *Cell* **185**, 4682–4702 (2022).
13. Achkar, J. M. & Jenny-Avital, E. R. Incipient and Subclinical Tuberculosis: Defining Early Disease States in the Context of Host Immune Response. *J. Infect. Dis.* **204**, S1179–S1186 (2011).
14. Tameris, M. et al. The Candidate TB Vaccine, MVA85A, Induces Highly Durable Th1 Responses. *PloS one* **9**, e87340 (2014).
15. Roy Chowdhury, R. et al. A multi-cohort study of the immune factors associated with M. tuberculosis infection outcomes. *Nature* **560**, 644–648 (2018).
16. Ribot, J. C. et al. CD27 is a thymic determinant of the balance between interferon-gamma- and interleukin 17-producing gammadelta T cell subsets. *Nat. Immunol.* **10**, 427–436 (2009).
17. Ribot, J. C., Lopes, N. & Silva-Santos, B. γδ T cells in tissue physiology and surveillance. *Nat. Rev. Immunol.* **21**, 221–232 (2021).
18. Roy Chowdhury, R. et al. NK-like CD8(+) γδ T cells are expanded in persistent Mycobacterium tuberculosis infection. *Sci. Immunol.* **8**, eade3525 (2023).
19. Peng, M. Y. et al. Interleukin 17-producing gamma delta T cells increased in patients with active pulmonary tuberculosis. *Cell Mol. Immunol.* **5**, 203–208 (2008).
20. White, A. D. et al. MTBVAC vaccination protects rhesus macaques against aerosol challenge with M. tuberculosis and induces immune signatures analogous to those observed in clinical studies. *NPJ Vaccines* **6**, 4 (2021).
21. Tarancon, R. et al. New live attenuated tuberculosis vaccine MTBVAC induces trained immunity and confers protection against experimental lethal pneumonia. *PLoS Pathog.* **16**, e1008404 (2020).
22. Esteso, G. et al. BCG-activation of leukocytes is sufficient for the generation of donor-independent innate anti-tumor NK and gammadelta T-cells that can be further expanded in vitro. *Oncoimmunology* **12**, 2160094 (2023).
23. Butler, A., Hoffman, P., Smibert, P., Papalexi, E. & Satija, R. Integrating single-cell transcriptomic data across different conditions, technologies, and species. *Nat. Biotechnol.* **36**, 411–420 (2018).
24. Singh, R., Kim, Y. H., Lee, S. J., Eom, H. S. & Choi, B. K. 4-1BB immunotherapy: advances and hurdles. *Exp. Mol. Med.* **56**, 32–39 (2024).
25. Kwon, B. S. et al. Immune responses in 4-1BB (CD137)-deficient mice. *J. Immunol.* **168**, 5483–5490 (2002).
26. Tang, R., Rangachari, M. & Kuchroo, V. K. Tim-3: A co-receptor with diverse roles in T cell exhaustion and tolerance. *Semin. Immunol.* **42**, 101302 (2019).
27. Muñoz-Ruiz, M. et al. IFN-γ-dependent interactions between tissue-intrinsic γδ T cells and tissue-infiltrating CD8 T cells limit allergic contact dermatitis. *J. Allergy Clin. Immunol.* **152**, 1520–1540 (2023).
28. Agerholm, R., Kadekar, D., Rizk, J. & Bekiaris, V. Type I interferon supports gammadelta T-cell homeostasis and immunity through direct and indirect receptor signaling in mice. *Eur. J. Immunol.* **51**, 3186–3193 (2021).
29. Vrieling, M., Santema, W., Van Rhijn, I., Rutten, V. & Koets, A. gammadelta T cell homing to skin and migration to skin-draining lymph nodes is CCR7 independent. *J. Immunol.* **188**, 578–584 (2012).
30. Thiele, D., La Gruta, N. L., Nguyen, A. & Hussain, T. Hiding in Plain Sight: Virtually Unrecognizable Memory Phenotype CD8(+) T cells. *Int. J. Mol. Sci.* **21**, 8626 (2020).
31. Louis, T. L. et al. Regulation of CD8 T Cell Differentiation by the RNA-Binding Protein DDX5. *J. Immunol.* **211**, 241–251 (2023).
32. Horenstein, A. L. et al. A CD38/CD203a/CD73 ectoenzymatic pathway independent of CD39 drives a novel adenosinergic loop in human T lymphocytes. *Oncoimmunology* **2**, e26246 (2013).
33. Ohta, A. et al. A2A adenosine receptor protects tumors from antitumor T cells. *Proc. Natl Acad. Sci. USA* **103**, 13132–13137 (2006).
34. Philip, M. et al. Chromatin states define tumour-specific T cell dysfunction and reprogramming. *Nature* **545**, 452–456 (2017).
35. Gowhari Shabgah, A. et al. A comprehensive review of IL-26 to pave a new way for a profound understanding of the pathobiology of cancer, inflammatory diseases and infections. *Immunology* **165**, 44–60 (2022).
36. Felgueres, M.-J. et al. BCG priming followed by a novel interleukin combination activates Natural Killer cells to selectively proliferate and become anti-tumour long-lived effectors. *Sci. Rep.* **14**, 13133 (2024).
37. Hoft, D. F., Brown, R. M. & Roodman, S. T. Bacille Calmette-Guérin Vaccination Enhances Human γδ T Cell Responsiveness to Mycobacteria Suggestive of a Memory-Like Phenotype1. *J. Immunol.* **161**, 1045–1054 (1998).

38. Eberl, M., Engel, R., Beck, E. & Jomaa, H. Differentiation of human γδ T cells towards distinct memory phenotypes. *Cell. Immunol.* **218**, 1–6 (2002).
39. Hu, Y. et al. γδ T cells: origin and fate, subsets, diseases and immunotherapy. *Signal Transduct. Target. Ther.* **8**, 434 (2023).
40. Li, P., Li, Y., Wang, C. C. & Xia, L. G. Comparative transcriptomics reveals common and strain-specific responses of human macrophages to infection with Mycobacterium tuberculosis and Mycobacterium bovis BCG. *Micro. Pathog.* **189**, 106593 (2024).
41. Lockhart, E., Green, A. M. & Flynn, J. L. IL-17 production is dominated by gammadelta T cells rather than CD4 T cells during Mycobacterium tuberculosis infection. *J. Immunol.* **177**, 4662–4669 (2006).
42. Caccamo, N. et al. Differentiation, phenotype, and function of interleukin-17-producing human Vγ9Vδ2 T cells. *Blood* **118**, 129–138 (2011).
43. Waldmann, T. A. The biology of interleukin-2 and interleukin-15: implications for cancer therapy and vaccine design. *Nat. Rev. Immunol.* **6**, 595–601 (2006).
44. Leonard, W. J., Lin, J. X. & O'Shea, J. J. The gamma(c) Family of Cytokines: Basic Biology to Therapeutic Ramifications. *Immunity* **50**, 832–850 (2019).
45. Ring, A. M. et al. Mechanistic and structural insight into the functional dichotomy between IL-2 and IL-15. *Nat. Immunol.* **13**, 1187–1195 (2012).
46. McNamara, M. J., Kasiewicz, M. J., Linch, S. N., Dubay, C. & Redmond, W. L. Common gamma chain (gammac) cytokines differentially potentiate TNFR family signaling in antigen-activated CD8(+) T cells. *J. Immunother. Cancer* **2**, 28 (2014).
47. Hogg, A. E., Bowick, G. C., Herzog, N. K., Cloyd, M. W. & Endsley, J. J. Induction of granulysin in CD8+ T cells by IL-21 and IL-15 is suppressed by human immunodeficiency virus-1. *J. Leukoc. Biol.* **86**, 1191–1203 (2009).
48. Zeng, R. et al. The molecular basis of IL-21-mediated proliferation. *Blood* **109**, 4135–4142 (2007).
49. Spolski, R. & Leonard, W. J. Interleukin-21: a double-edged sword with therapeutic potential. *Nat. Rev. Drug Discov.* **13**, 379–395 (2014).
50. Wolf, Y., Anderson, A. C. & Kuchroo, V. K. TIM3 comes of age as an inhibitory receptor. *Nat. Rev. Immunol.* **20**, 173–185 (2020).
51. Jayaraman, P. et al. Tim3 binding to galectin-9 stimulates antimicrobial immunity. *J. Exp. Med* **207**, 2343–2354 (2010).
52. Tippalagama, R. et al. HLA-DR Marks Recently Divided Antigen-Specific Effector CD4 T Cells in Active Tuberculosis Patients. *J. Immunol.* **207**, 523–533 (2021).
53. Alvarez-Arguedas, S. et al. Therapeutic efficacy of the live-attenuated Mycobacterium tuberculosis vaccine, MTBVAC, in a preclinical model of bladder cancer. *Transl. Res* **197**, 32–42 (2018).
54. Felgueres, M.-J., Esteso, G., Aguiló, N. & Valés-Gómez, M. Selective expansion of anti-tumor innate lymphocytes in long-term cultures after a single BCG pulse. *Methods Cell Biol*. **190**, 203–221 (2024).
55. Bryceson, Y. T. et al. Functional analysis of human NK cells by flow cytometry. *Methods Mol. Biol.* **612**, 335–352 (2010).

Acknowledgements

The group of MVG belongs to the research network Cancer hub-CSIC and to the EU-COST action IMMUNO-model. M.J.F. and A.F.G.J. were registered PhD students at the Molecular Biosciences doctoral program of the Universidad Autónoma de Madrid (UAM).This study was funded by grants RTC-2017-6379-1, PID2021-123795OB-I00 (MVG) and PID2020-115506RB-I00 (HTR), by MICIU/AEI/ 10.13039/501100011033 and by "ERDF A way of making Europe"; Grant FPU18/01698 (AFGJ) by MICIU/AEI/ 10.13039/501100011033 and by "ESF Investing in your future" (ESF+); INPhINIT Doctoral Programme from La Caixa Foundation LCF/BQ/DI19/ 11730039 (MJF); MVG acknowledges financial support from the Spanish State Research Agency, AEI/10.13039/501100011033, through the "Severo Ochoa" Program for Centres of Excellence in R&D [CEX2023-001386-S]. Funders played no role in study design, data collection, analysis and interpretation of data, or the writing of this manuscript.

Author contributions

M.J.F., A.F.G.J., G.E., N.A., and M.V.G. acquired, analysed, and interpreted data. N.A., A.D., E.P., I.M., C.M., E.R., H.T.R. and M.V.G. provided reagents and material support. A.B., E.V. performed scRNAseq analysis and curated data. M.V.G. supervised the study. M.J.F. and M.V.G. and wrote the manuscript with critical revisions by all authors.

Competing interests

C.M., N.A., E.R. and E.P. are co-inventors of the patent "tuberculosis vaccine" filled by the University of Zaragoza and Biofabri. Biofabri is industrial manufacturer and exclusive licensee of MTBVAC. E.P., I.M., E.R. are Biofabri's employees. The rest of the authors declare no competing financial interests.

Additional information

Supplementary information The online version contains supplementary material available at https://doi.org/10.1038/s41541-025-01110-3.

Correspondence and requests for materials should be addressed to Mar Valés-Gómez.